Supporting Information

Amphitrite ornata Dehaloperoxidase (DHP): Investigations of Structural Factors that Influence the Mechanism of Halophenol Dehalogenation using "Peroxidase-Like" Myoglobin Mutants and "Myoglobin-Like" DHP Mutants[†‡]

Jing Du,[§,‖] *Xiao Huang,*[§,‖] *Shengfang Sun,*[§] *Chunxue Wang,*[§] *Lukasz Lebioda,*[*§] *and John H. Dawson*[*§,⊥]

[§] Department of Chemistry and Biochemistry, University of South Carolina, Columbia, South Carolina 20208,[⊥] School of Medicine, University of South Carolina,

* To whom correspondence should be addressed: Department of Chemistry and Biochemistry, 631 Sumter St., University of South Carolina, Columbia, SC 29208. Phone: (803) 777-2414 or (803) 777-7234. Fax: (803)777-9521. E-mail: lebioda@mail.chem.sc.edu, or dawson@sc.edu

[†] Financial support provided by the National Science Foundation (MCB 0820456).

[‖] These authors contributed equally.

[‡] Crystal coordinates for G65T and G65I variants of sperm whale myoglobin mutants have been deposited in the Protein Data Bank as entries 3OCK and 3SDN, respectively. Data were collected at the SER-CAT 22-ID and 22-BM beamlines at the Advanced Photon Source, Argonne National Laboratory. Use of the Advanced Photon Source was supported by the U. S. Department of Energy, Office of Basic Energy Sciences, under Contract No. W-31-109-Eng-38.

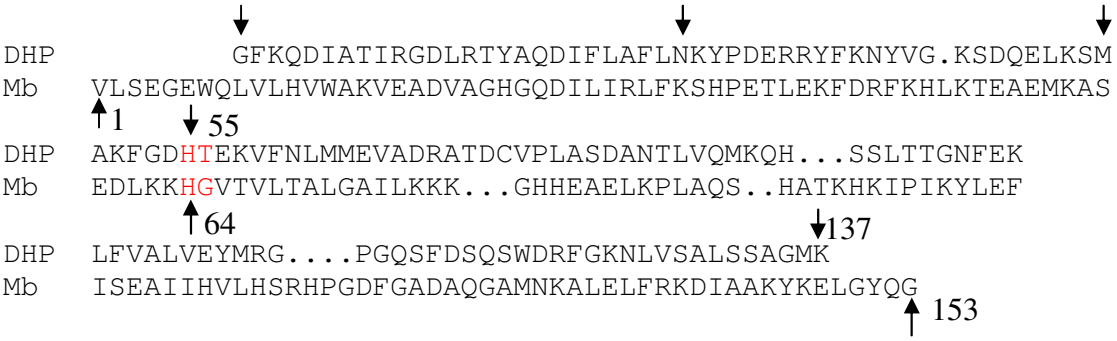

Scheme S1. The alignment of Mb and DHP amino acid sequences.

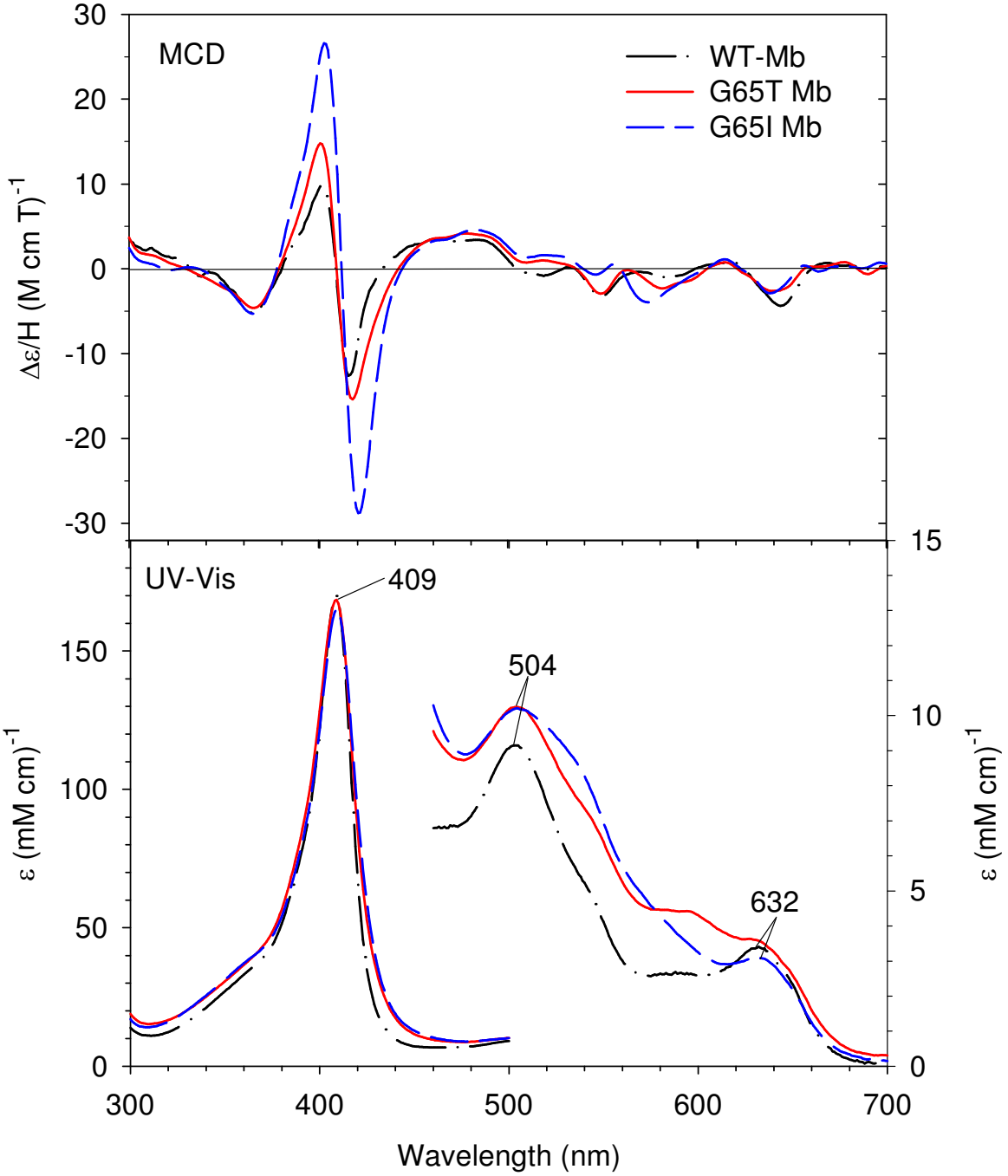

Figure S1. MCD (top) and UV-Vis (bottom) absorption spectra of ferric wild-type (dash-dotted line), G65T (solid line) and G65I Mb mutants (dashed line) in 0.1 M potassium phosphate buffer pH 7.

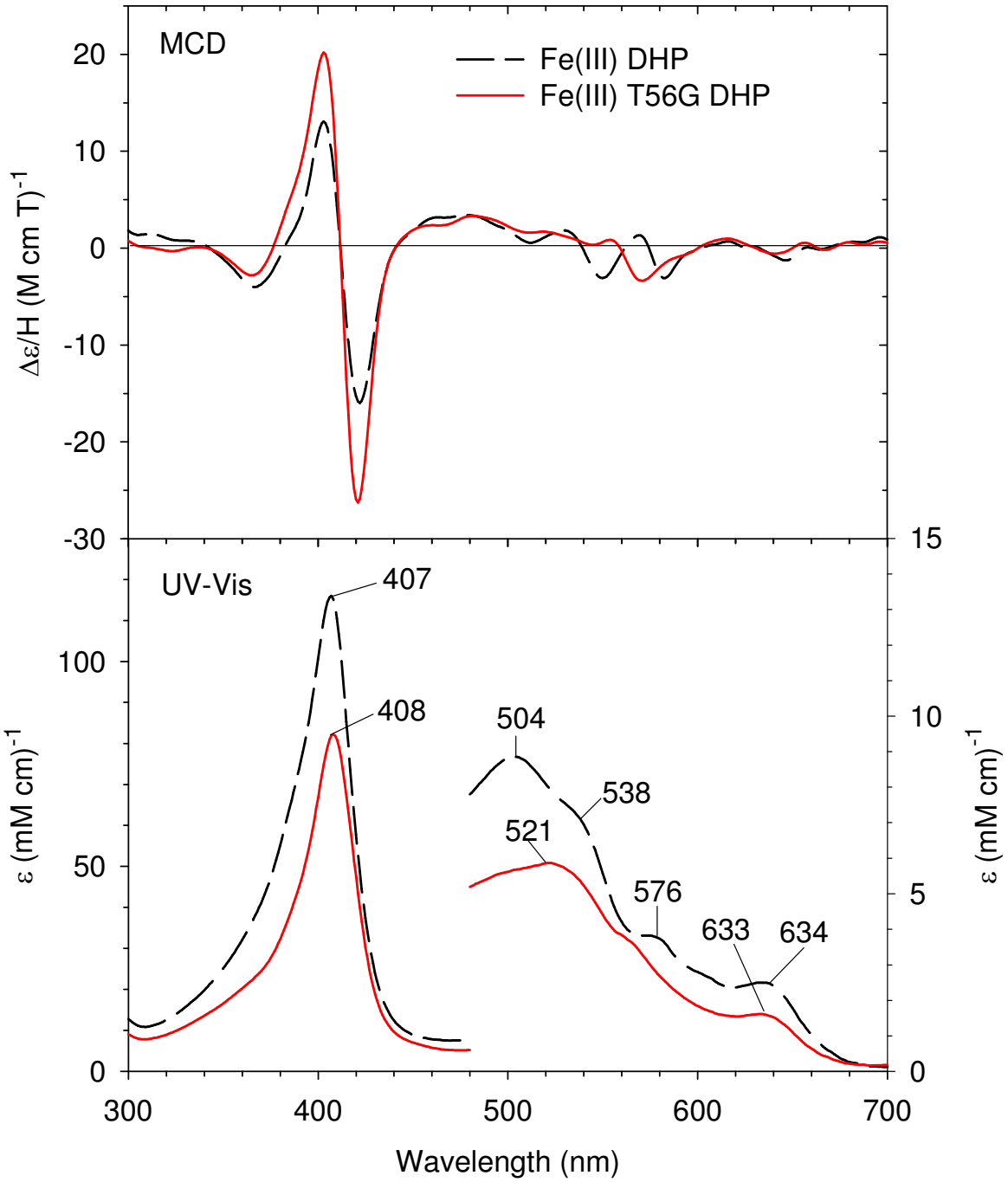

Figure S2. MCD (top) and UV-Vis (bottom) absorption spectra of ferric wild-type (dashed line) and T56G DHP mutant (solid line) in 0.1 M potassium phosphate buffer pH 7.

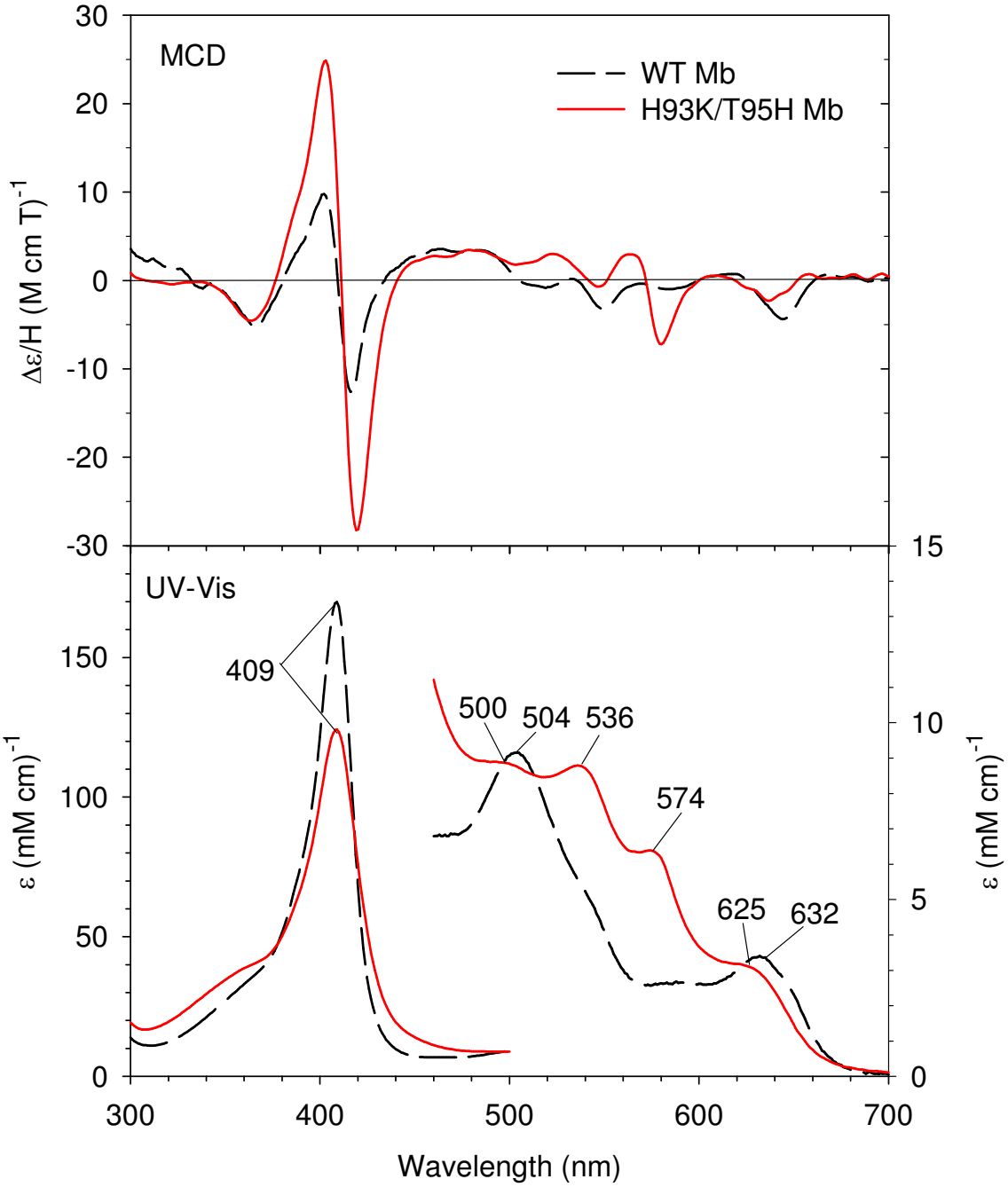

Figure S3. MCD (top) and UV-Vis (bottom) absorption spectra of ferric wild-type (dashed line) and H93K/T95H Mb mutant (solid line) in 0.1 M potassium phosphate buffer pH 7.

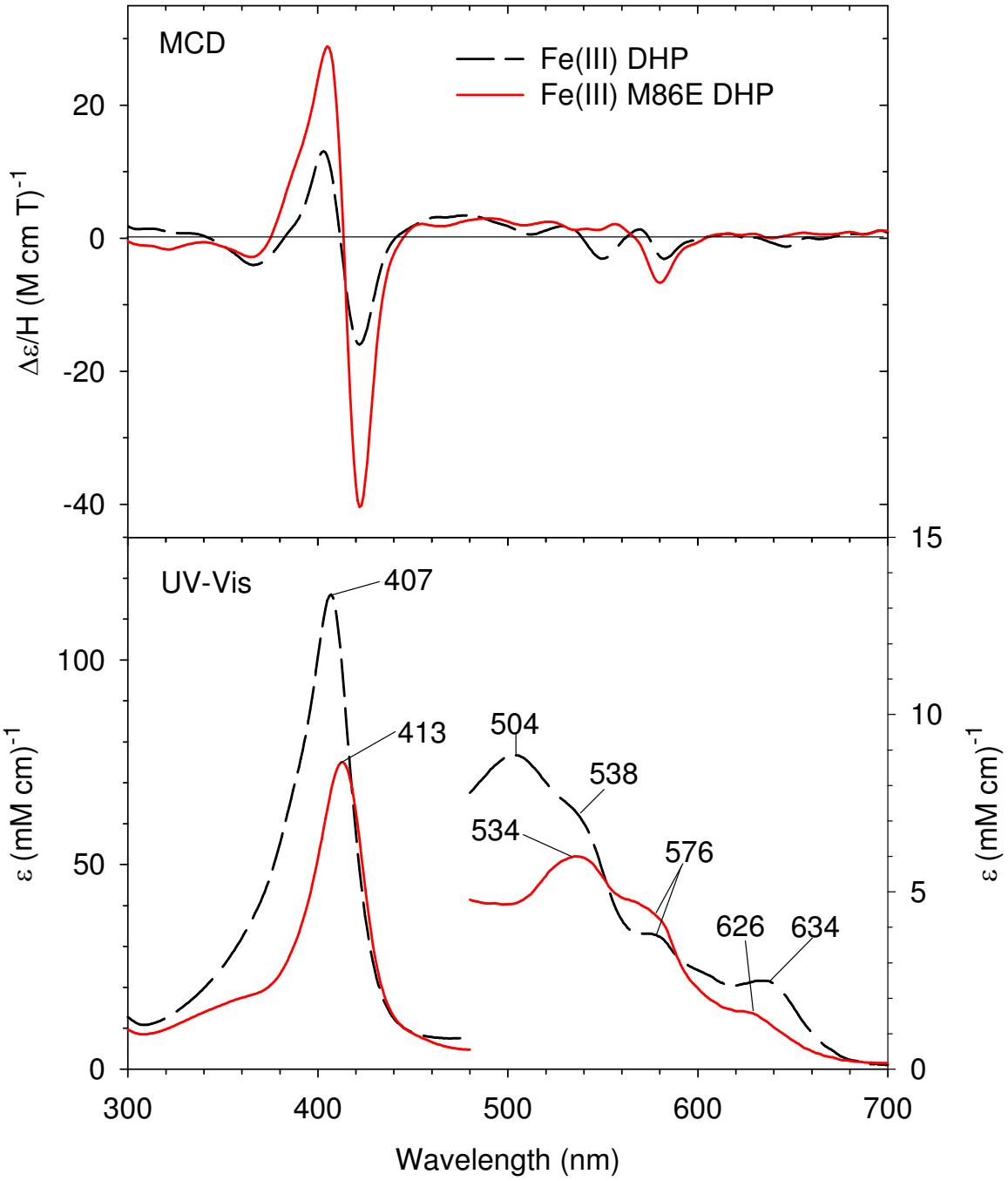

Figure S4. MCD (top) and UV-Vis (bottom) absorption spectra of ferric wild-type (dashed line) and M86E mutant DHP (solid line) in 0.1 M potassium phosphate buffer pH 7.

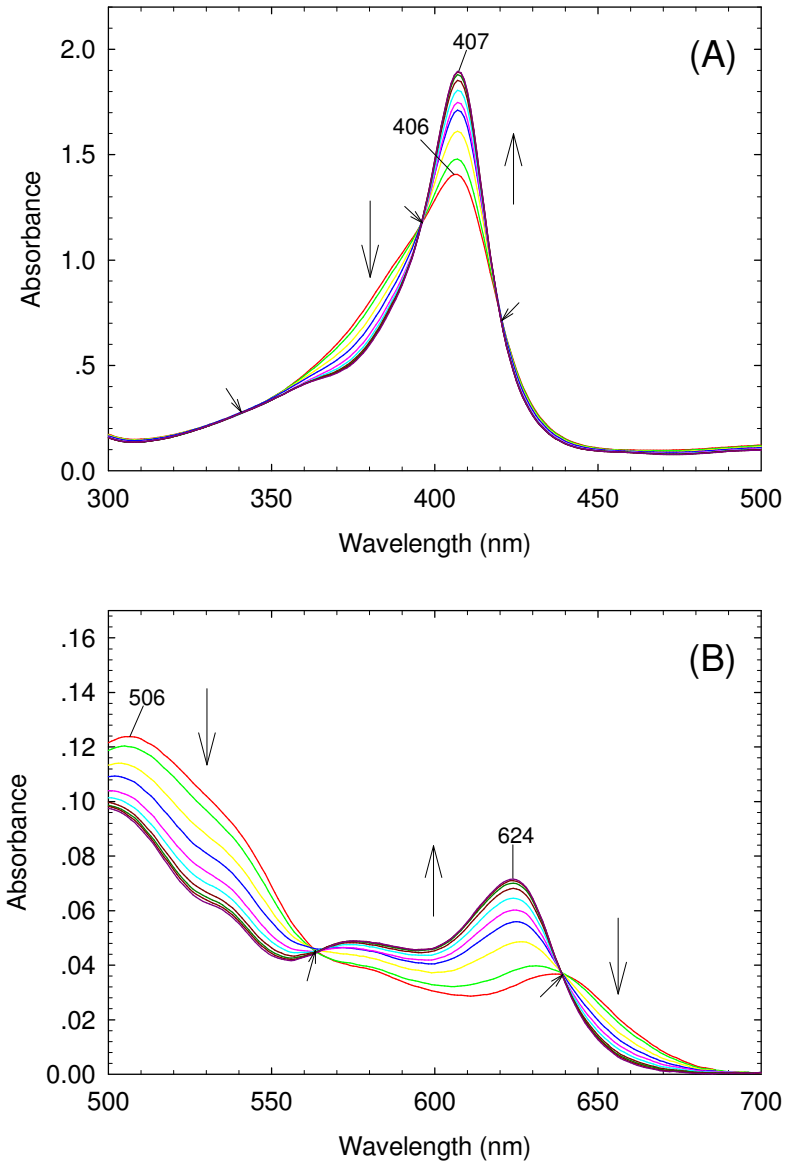

Figure S5. (A) Soret region and (B) visible region absorption spectral changes upon titration of exogenous ligand-free ferric DHP (65 μM in a 0.2-cm cuvette) with sodium acetate in 50 mM sodium citrate buffer, pH 5.4, at 4 °C. Vertical arrows indicate the directions of absorbance change on addition of 0, 0.3, 0.6, 1.1, 2.8, 5.5, 11.0, 22.0, 43.0 and 82.0 mM sodium acetate. The non-vertical short arrows show isosbestic points.

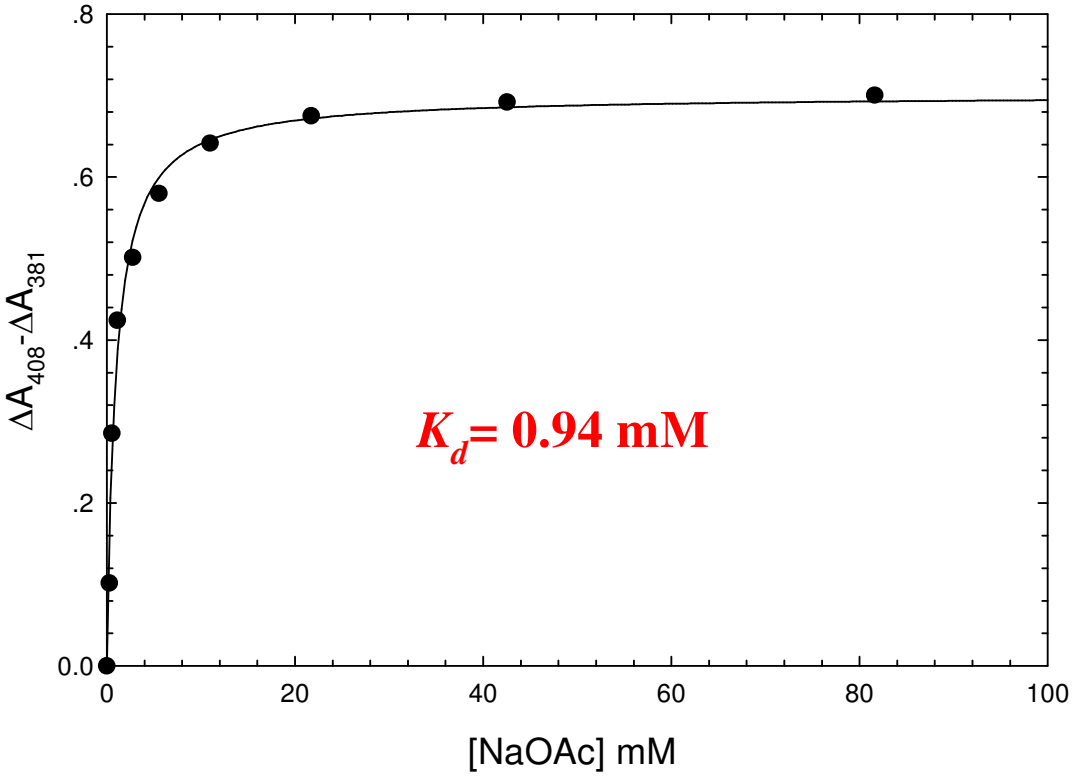

Figure S6. Hyperbolic saturation plots of sodium acetate titration results shown in Figure S5 for acetate binding to exogenous ligand-free ferric DHP. Maximum absorbance changes in difference spectra (not shown) in the Soret region are plotted as a function of total ligand concentration. Lines drawn are non-linear fits for a bimolecular association model to the data.

Table S1. Turnover numbers for the oxidative dechlorination of 150 μM TCP with DHP and varying H_2O_2 concentration in 50 mM sodium citrate buffer pH 5.4 or 50 mM sodium acetate buffer pH 5.4 at 4 °C.

Protein (4 °C)	buffer	Formula	k_{cat} (mol Prod)(mol ENZ)$^{-1}$min^{-1}
DHP	sodium acetate buffer pH 5.4	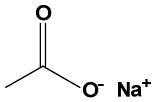	198± 1
	sodium citrate buffer pH 5.4	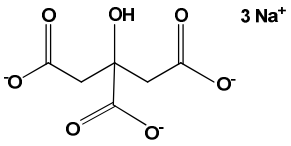	243 ± 3

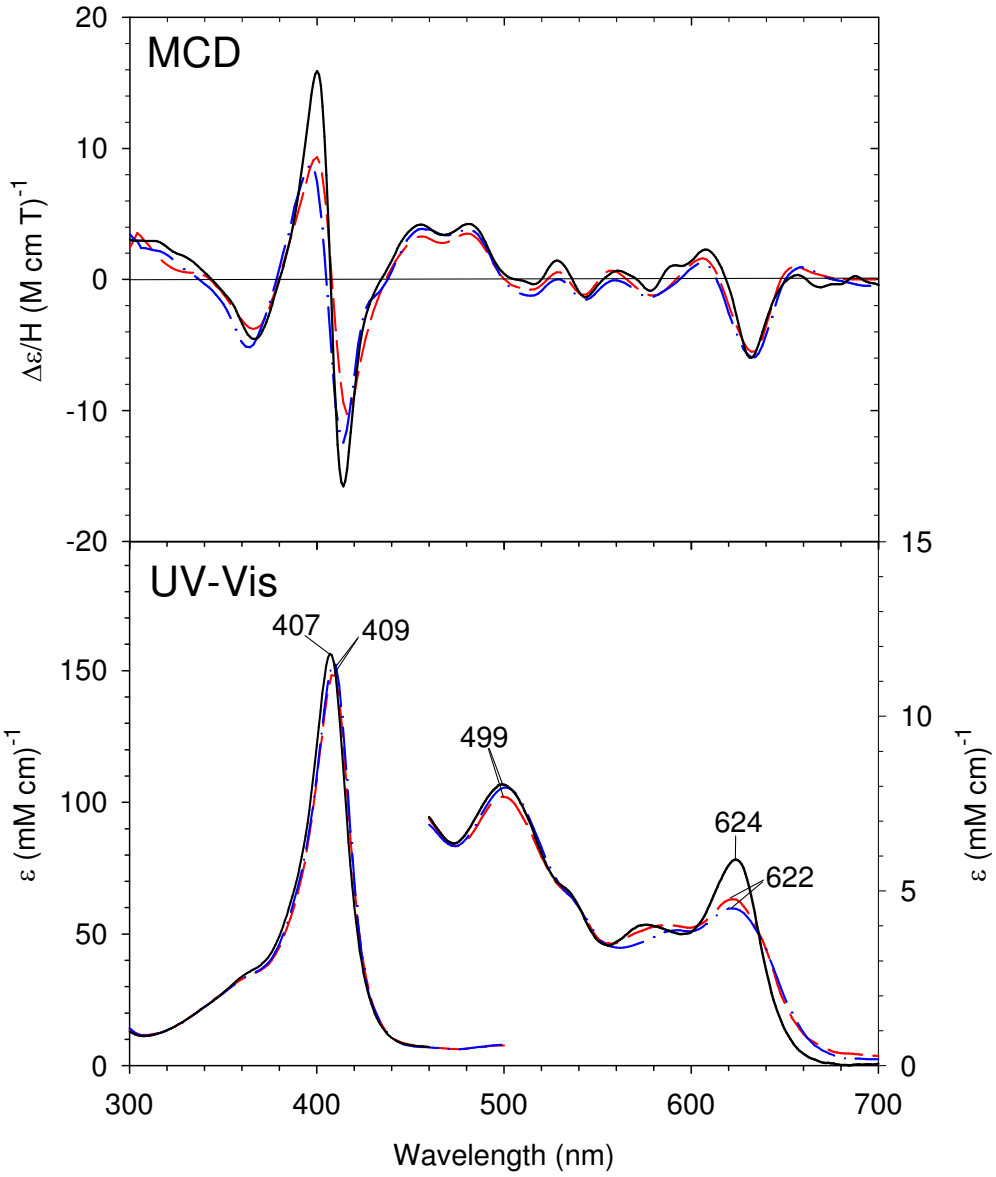

Figure S7. MCD (top) and UV-Vis (bottom) absorption spectra of ferric acetate-bound DHP (solid line, 82 mM) in 50 mM sodium citrate buffer, pH 5.4, at 4 °C, ferric acetate-bound Mb (dashed line, 6 M sodium acetate) and ferric formate-bound Mb (dash-dotted line, 1 M sodium formate) in 0.1 M potassium phosphate buffer pH 7. [The spectra of the acetate- and formate-Mb complexes were provided by Dr. M. Sono (M. Sono, J.H. Dawson, unpublished data).]

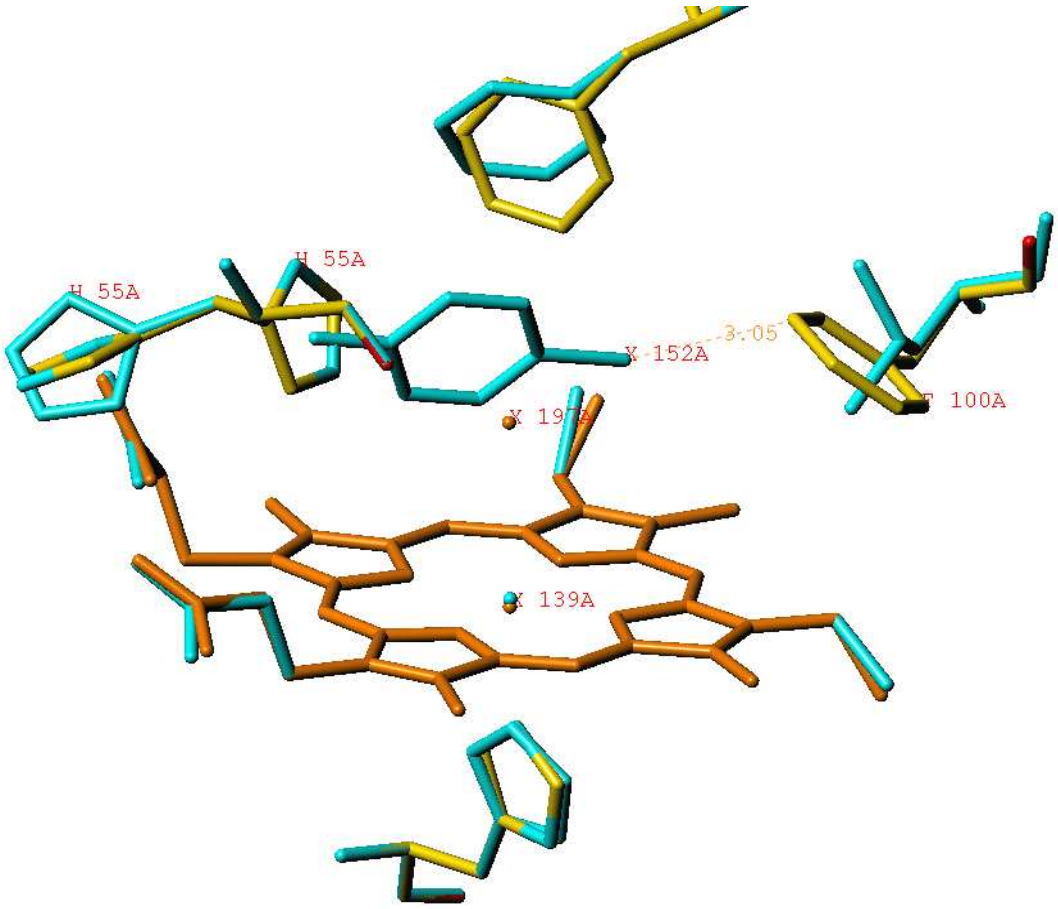

Figure S8. Superposition of the crystal structures of wild-type DHP (cyan) with the simulated configuration L100F mutant (yellow). The common porphyrin atoms are shown in orange. Modeling indicates that the larger side chain of Phe in position 100 can be accommodated in the cavity but it would "push out" the iodophenol molecule by about 1.2 Å.

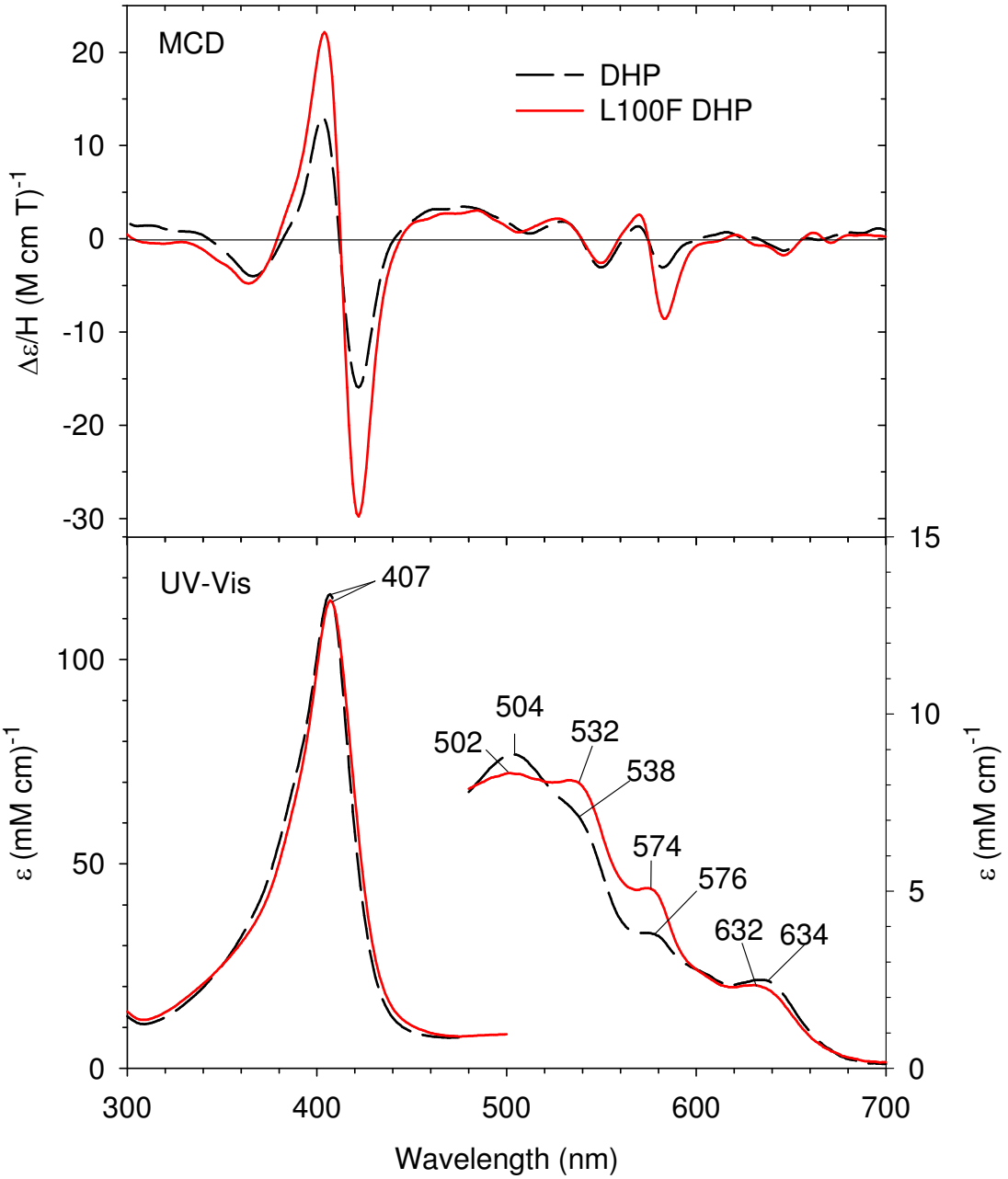

Figure S9. MCD (top) and UV-Vis (bottom) absorption spectra of ferric wild-type (dashed line) and L100F mutant DHP (solid line) in 0.1 M potassium phosphate buffer pH 7.

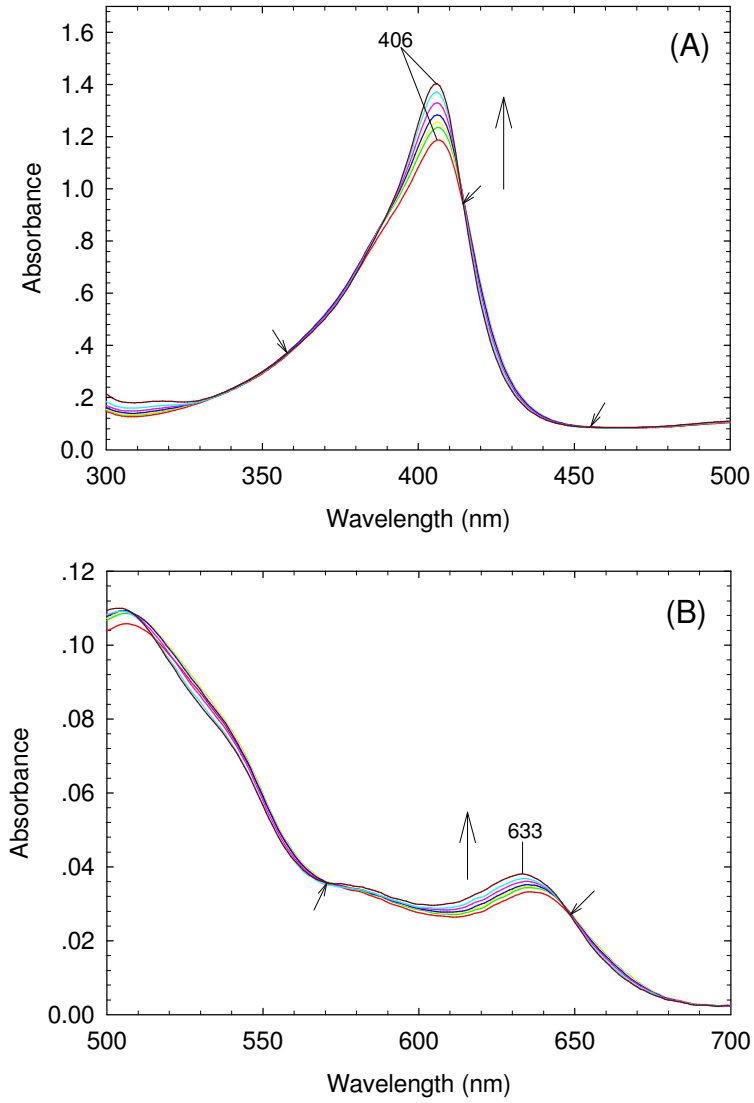

Figure S10. (A) Soret region and (B) visible region absorption spectral changes upon titration of exogenous ligand-free ferric DHP (50 μM in a 0.2-cm cuvette) with TCP in 50 mM sodium citrate buffer, pH 5.4, at 4 °C. Vertical arrows indicate the directions of absorbance change on addition of 0, 5, 10, 20, 40, 80 and 160 μM TCP. The non-vertical short arrows show isosbestic points.

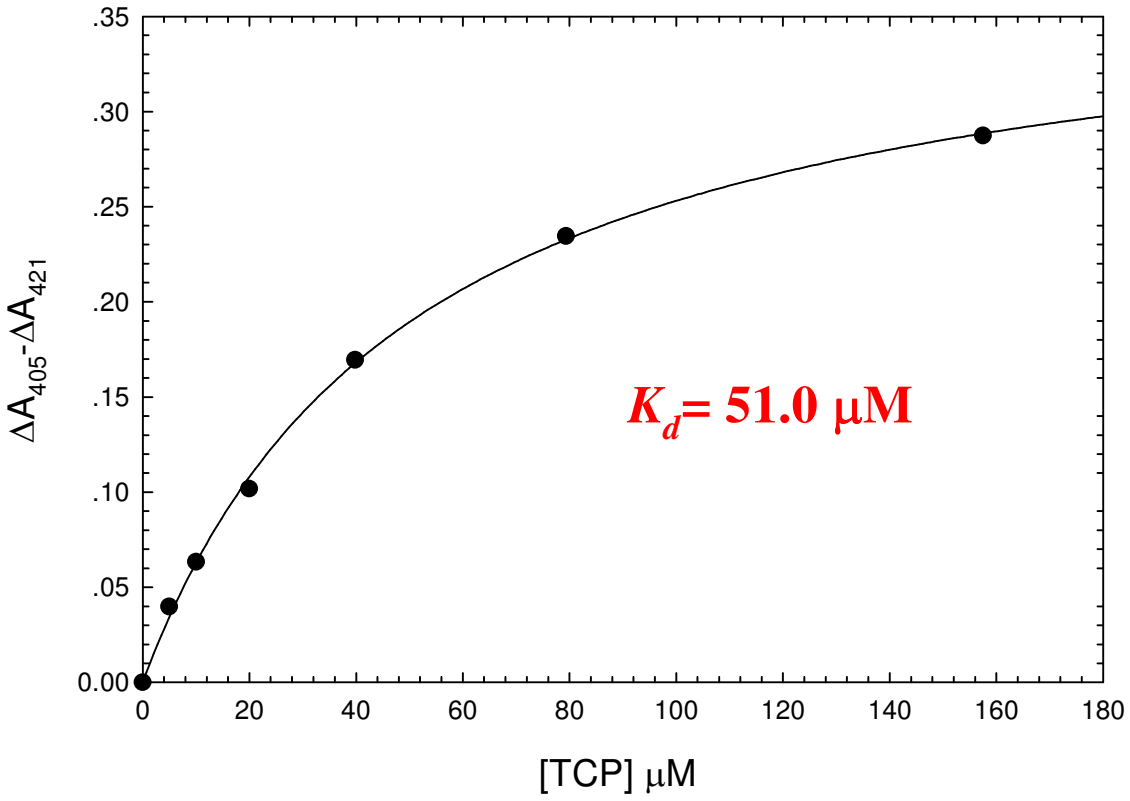

Figure S11. Hyperbolic saturation plots of TCP titration results shown in Figure S10 for TCP binding to exogenous ligand-free DHP. Maximum absorbance changes in difference spectra (not shown) in the Soret region are plotted as a function of total TCP concentration. Lines drawn are non-linear fits for a bimolecular association model to the data.

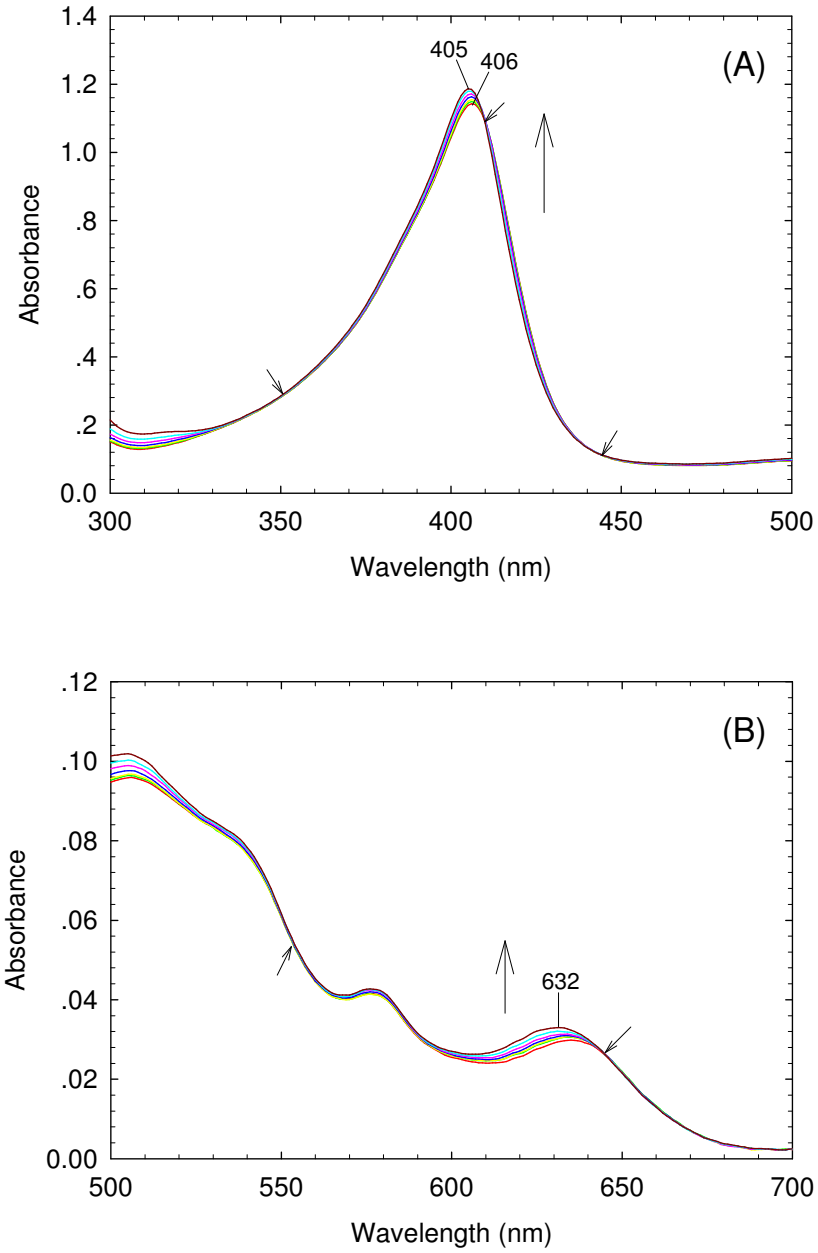

Figure S12. (A) Soret region and (B) visible region absorption spectral changes upon titration of exogenous ligand-free ferric L100F DHP mutant (50 μM in a 0.2-cm cuvette) with TCP in 50 mM sodium citrate buffer, pH 5.4, at 4 °C. Vertical arrows indicate the directions of absorbance change on addition of 0, 5, 10, 20, 40, 80 and 160 μM TCP. The non-vertical short arrows show isosbestic points.

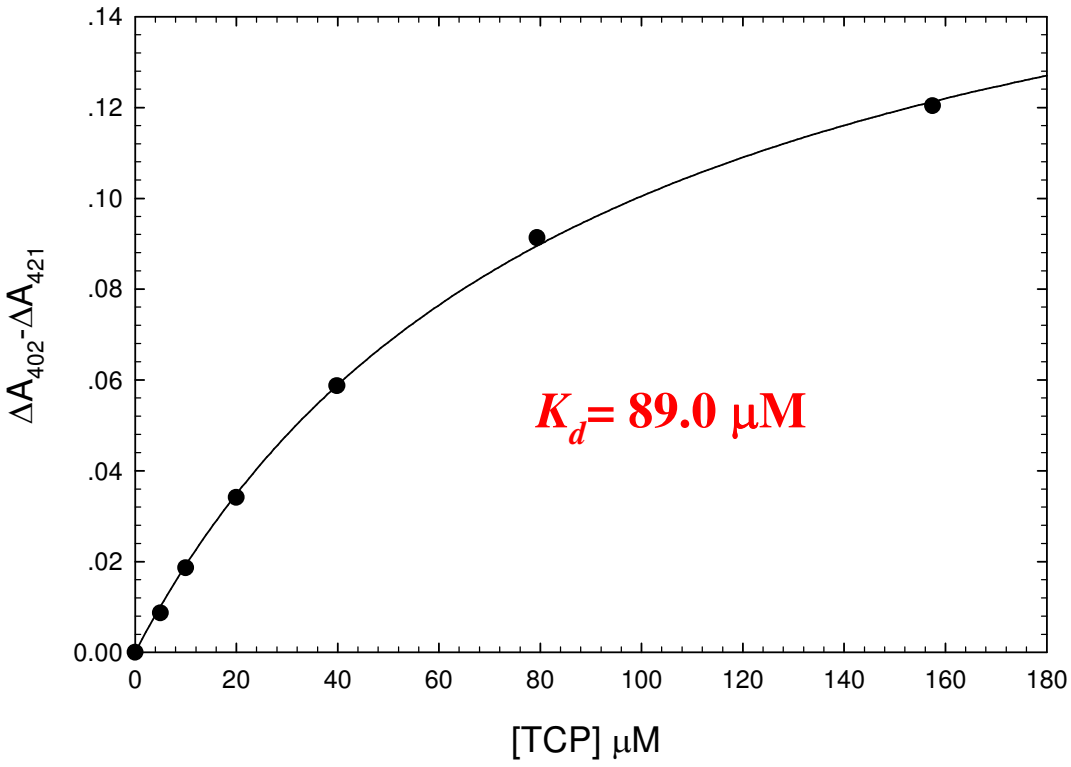

Figure S13. Hyperbolic saturation plots of TCP titration results shown in Figure S12 for TCP binding to exogenous ligand-free L100F DHP mutant. Maximum absorbance changes in difference spectra (not shown) in the Soret region are plotted as a function of total TCP concentration. Lines drawn are non-linear fits for a bimolecular association model to the data.